# Imaging performance comparison between CMOS and sCMOS detectors in a vibration test on large areas using digital holographic interferometry

J. M. Flores-Morenoa, Manuel H. De la Torre I., Daniel D. Aguayo, and Fernando Mendoza S.

Citation: AIP Conference Proceedings **1600**, 223 (2014); doi: 10.1063/1.4879586
View online: http://dx.doi.org/10.1063/1.4879586
View Table of Contents: http://scitation.aip.org/content/aip/proceeding/aipcp/1600?ver=pdfcov
Published by the AIP Publishing

**Articles you may be interested in**

Imaging performance of amorphous selenium based flat-panel detectors for digital mammography: Characterization of a small area prototype detector
Med. Phys. **30**, 254 (2003); 10.1118/1.1538233

Largearea, freestanding gratings for atom interferometry produced using holographic lithography
J. Vac. Sci. Technol. B **10**, 2909 (1992); 10.1116/1.585986

Holographic interferometry of vibrating objects
Phys. Teach. **30**, 219 (1992); 10.1119/1.2343523

Using holographic interferometry in vibration measurements
J. Acoust. Soc. Am. **74**, S14 (1983); 10.1121/1.2020819

Vibration Analysis by Holographic Interferometry
J. Acoust. Soc. Am. **44**, 1225 (1968); 10.1121/1.1911251

This article is copyrighted as indicated in the article. Reuse of AIP content is subject to the terms at: http://scitation.aip.org/termsconditions. Downloaded to IP: 200.23.6.133 On: Thu, 03 Jul 2014 22:40:27

# Imaging performance comparison between CMOS and sCMOS detectors in a vibration test on large areas using digital holographic interferometry

J.M. Flores-Moreno[a], Manuel H. De la Torre I. [a], Daniel D. Aguayo[b], Fernando Mendoza S.[a]

[a]*Centro de Investigaciones en Óptica, A.C., Loma Del Bosque 115, León Guanajuato C.P. 37150, México*
[b]*Antwerpen University, Laboratory of Biomedical, Groenenborgerland 171 B-2020 Belgium*

**Abstract.** A comparison of the interferometric imaging performance of two different cameras during a vibration study is presented. One of the cameras has a high speed CMOS sensor and the second one uses a high resolution (scientific) sCMOS sensor. This comparison is based on the interferometric response as a merit parameter of these sensors which is not a conventional procedure. Even when the current standard for image quality is on the signal to noise ratio calculations, an interferometric test to evaluate the fringe pattern visibility is equivalent to the contrast to noise ratio value. An out of plane digital holographic interferometer is used to test each camera once at the time with the same experimental conditions. The object under study is a metallically framed table with a Formica cover with an observable area of 1.1 $m^2$. The sample is deformed by means of a controlled vibration induced by a tip ended linear step motor. Results from each camera are presented as the retrieved optical phase during the vibration. Finally, some conclusions based on the post processed images are presented suggesting a smoother optical phase obtained with the sCMOS camera.

**Keywords:** Interferometry, digital holographic interferometry, imaging detectors.
**PACS:** 42.25.Hz, 42.40.Kw, 42.79.Pw.

## INTRODUCTION

The imaging sensors are essential tools in almost any science where the image registrations from different tests are required. Modern detectors shown several advantages compared with the human eye [1], such as the spectral sensitivity in a range coming from the x-ray until the infrared wavelengths. Extended technology in image sensors involved the manufacturing of charged coupled devices (CCD) and complementary metal oxide semiconductor (CMOS) ones [2, 3]. The state of the art of recent imaging detectors explores their applicability into low light environments, making them suitable in life science imaging. At the top of the high performance sensors are the electron multiplying CCDs (EM-CCDs) and the scientific CMOS (sCMOS), both representing a breakthrough of on-chip imaging technology [4]. Recent review articles, technical whitepapers and scientific reports discuss the merits of the sCMOS and the EM-CCD cameras technology mainly focused in the biological microscopy field [5-7], the astronomical observation [8], and the technical advantages or drawbacks between them [4, 9, 10]. All these studies and comparisons are based mainly in the quantification of the signal to noise ratio (SNR) under specific illumination conditions, optical configurations and background noise. Only few manuscripts have been reported applying interferometric techniques to evaluate the performance of the imaging detectors [11, 12]. They are based on the calculation of the modulation transfer function (MTF) and power spectral density (PSD) as quality parameters to evaluate the recorded images. The last work measures the MTF using a double-slit aperture to generate the speckle phenomenon by an integrating sphere.

In this manuscript, we propose an interferometric technique to compare the performance of two imaging sensors: a CMOS camera (PCO DIMAX HD+ with 1920 X 1440 pixels at 12 bits) and a sCMOS camera (PCO EDGE with 1920 X 1080 pixels at 12 bits). In this report we are not using an EM-CCD sensor in order to compare only two

*11th International Conference on Vibration Measurements by Laser and Noncontact Techniques - AIVELA 2014*
AIP Conf. Proc. 1600, 223-227 (2014); doi: 10.1063/1.4879586
© 2014 AIP Publishing LLC 978-0-7354-1234-7/$30.00


This article is copyrighted as indicated in the article. Reuse of AIP content is subject to the terms at: http://scitation.aip.org/termsconditions. Downloaded to IP: 200.23.6.133 On: Thu, 03 Jul 2014 22:40:27

different CMOS configurations. The CMOS technology has been widely used in interferometry since it allows a faster acquisition rate applied in deformations and vibration modes over surfaces excited by controlled deformations [13, 14]. Nevertheless, this technology is related with a readout noise which appears as noisy wrapped phase maps in some interferometric applications. The sCMOS sensor improves the classical drawback associated to CMOS technology (i.e. high read noise, high dark current and lower fill factors) enhancing its performance and making it competitive even with the latest CCD technology (EM-CCD).

In the present work a large sample is illuminated in order to create extreme conditions where the optical phase can easily be affected due the extensive surface. Under this scenario, the same digital holographic interferometer (DHI) is used to registers the optical phase with two different cameras once at the time. In both cases the same deformation is applied to the sample and the images are recorded at 100 frames per second (fps). A brief description of the method is explain under the current setup configuration. Results from both cameras are shown as wrapped phase maps and a discussion concerning them is also included before the conclusions.

## METHODS

DHI is a non-invasive, remote and full field of view optical technique based on the two beam interference principle widely used for the study of vibrating objects. When the superposition of the backscattered light from the object´s surface and the reference beam is recorded by a 2D photo detector arrangement (either CCD or CMOS sensor), an image hologram is then recorded. Further processing of this image hologram retrieves the optical phase information embedded in it. The relative wrapped phase map represents the deformation between two different states of the object, i.e. the reference state and the deformed one. DHI can be applied to estimate several mechanical parameters from a sample, such as the displacement, stiffness (relative to a known applied force), the elastic modulus, the strain concentrators and the stress [15, 16]. The use of high speed cameras in DHI avoids the formation of Bessel fringes normally present with camera´s slow integration times. Instead of this, the high speed recording keeps a cosine profile that allows the use of the same methodology of traditional DHI to retrieve the optical phase [17]. Under this assumption, the wrapped phase map can be calculated using the following expression after a band pass filter [18],

$$\Delta\varphi_n = \operatorname{atan}\left[\frac{\mathrm{Re}(I_{n-1})\,\mathrm{Im}(I_n) - \mathrm{Im}(I_{n-1})\,\mathrm{Re}(I_n)}{\mathrm{Im}(I_{n-1})\,\mathrm{Re}(I_n) + \mathrm{Re}(I_{n-1})\,\mathrm{Im}(I_n)}\right] \quad (1),$$

where $\Delta\varphi n$ is the relative phase map between the nth and the nth-1 state, and terms Re and Im are the real and the imaginary parts of the complex data for each transformed image hologram. Since the calculated wrapped phase map is codified with values between $-\pi$ and $\pi$ (black and white respectively), an unwrapping algorithm is used to represent a continuous phase map which can be transformed into a displacement map with,

$$\Delta\varphi_n(x,y) = \frac{2\pi}{\lambda}(1+\cos\theta)w(x,y) \quad (2),$$

where w is the out of plane displacement, $\lambda$ is the laser wavelength and $\theta$ is the angle between the illumination and the observation directions.

## EXPERIMENTAL DESCRIPTION

In Fig.1 an schematic view of the optical system is shown. The laser beam coming from a Verdi V10 laser is split into the object and the reference beams by means of a right angle prism (BS). The reason to use a right angle prism instead of a cube beam splitter is the high output power of the laser, which would easily damage the union layer of the cube. The object beam is re-directed into the object´s surface using a couple of high power reflective mirrors (M1 and M2). This beam is then expanded to illuminate the entire object´s surface using a high numerical aperture (NA) lens (MO). The object´s backscattering is focused into the camera sensor by a lens (L) with a focal length of 60 mm, which has a rectangular aperture (A) next to it. A beam combiner (BC) in front of the camera helps to introduce the reference beam coming from a single mode optical fiber (OF) into the camera sensor together with the object´s backscattering. As a consequence, an interference pattern from the reference and the object beams is recorded by the camera.


This article is copyrighted as indicated in the article. Reuse of AIP content is subject to the terms at: http://scitation.aip.org/termsconditions. Downloaded to IP: 200.23.6.133 On: Thu, 03 Jul 2014 22:40:27

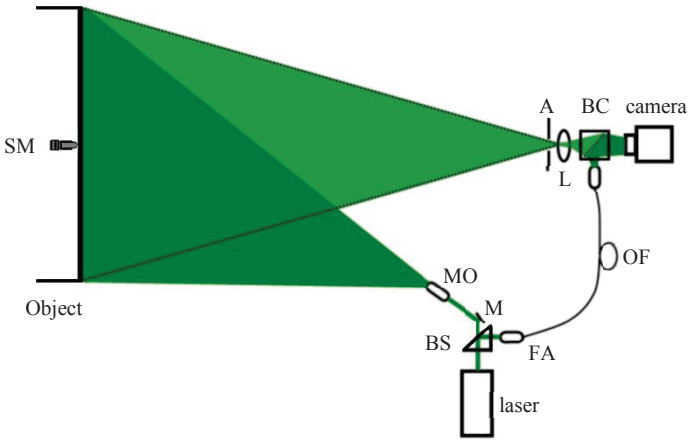


Figure 1. DHI optical setup in an schematic view.

The object under study is a metallically framed working table with a Formica layer cover with dimensions of 1.51 × 0.76 meters. The metallic frame is behind the observable area of the table, and it is mechanically connected with its four legs. This solid structure helps to reduce mechanical random movement during the test. Nevertheless, one of the major issues in the analysis of extensive areas is the need to take the remote inspection as far as several meters (6.5m in this case). The recording process is performed at 100 fps to avoid environmental noise and long stabilization times. Once the sample is properly focused and placed in front of the optical system, two tests are performed (i.e. one for each camera). When two different sensors are tested, it is important to keep the same experimental settings for each one such as, the illumination flux, the optical setup or the environmental conditions; a feature achieved during the tests.

In order to compare both camera sensors, appropriated optical adjustments should be made to project equivalent photons per pixel on the sensor with different pixel sizes. Typically, cameras with larger pixel sizes will collect more photons and show higher SNR than those with smaller pixel sizes (mainly in low light illumination). Several studies on the performance of sensors have been reported in this matter [4, 10]. Nevertheless, in our experimental setup a large object´s area is uniformly illuminated using a high power continuous laser which guarantees same average photons arriving to each sensor at each individual pixel. Although the pixel size is a critical parameter under low illumination conditions due the amount of photons per unit area converted in electrons, at high and constant illumination any sensor shows a similar SNR response [4] despite its pixel size.

## RESULTS

The vibration applied to the sample (at the back side of the table) by the SM generates complex fringe patterns on the large surface sample in order to test the performance of these two detectors. Figures 2 and 3 show the optical phase retrieved during the same vibration by the CMOS and the sCMOS detectors respectively. In these images it is possible to appreciate a single load and unload process coming from the SM´s tip. As it can be observed in these two wrapped phase map sequences, the sCMOS camera retrieves a smooth optical phase all over the table´s surface while the CMOS shows some optical de-correlation near the edges.

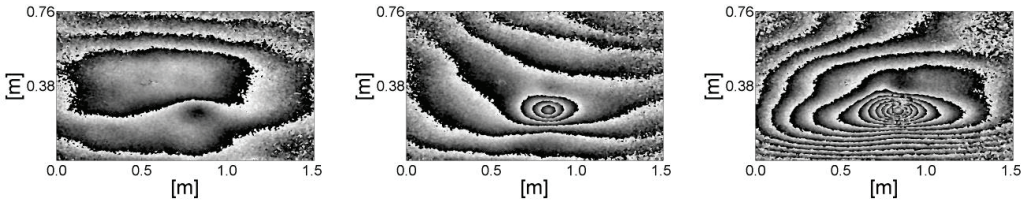


(a) (b) (c)



This article is copyrighted as indicated in the article. Reuse of AIP content is subject to the terms at: http://scitation.aip.org/termsconditions. Downloaded to IP: 200.23.6.133 On: Thu, 03 Jul 2014 22:40:27

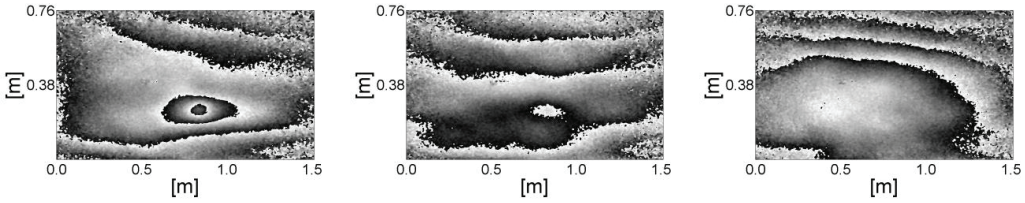


(d) (e) (f)

Figure 2. Wrapped phase maps obtained with the CMOS camera.

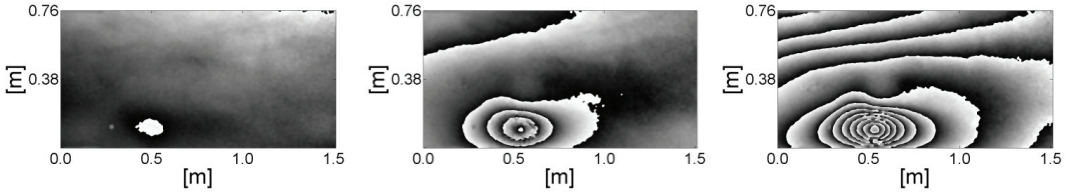


(a) (b) (c)

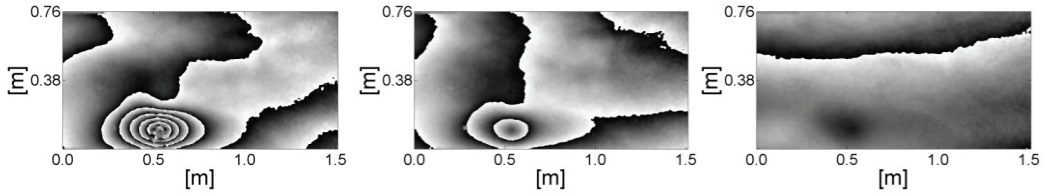


d) (e) (f)

Figure 3. Wrapped phase maps obtained with the sCMOS camera.

Both sequences are obtained with the same illumination condition, the same deformation induced and the same optical system (except by the camera used for each case). These results make evident the image enhancement of the sCMOS camera respect to the CMOS in this interferometric test. The importance to retrieve a smooth optical phase in vibration analysis without the need of pulsed lasers or synchronization systems is to study complex, non repeatable and non controlled events.

Besides, the possibility to obtain smooth displacement maps maintains the full field inspection advantage of this optical technique. This advantage creates dynamic and high SNR displacement maps from which it is possible to gather point wise information even at the edges of the sample. The sCMOS sensor obtains high visibility fringe patterns all over the object´s surface which allows further processing for low noise strain maps.

## CONCLUSIONS

We introduce a comparison to retrieved optical phase between a CMOS and a sCMOS detector under an interferometric test. When the optical phase maps obtained with the CMOS sensor are compared with those acquired with the sCMOS sensor, it is clear that no de-correlation is present in them meaning that the system is capable to define the close fringe clusters formed due to the excitation signal. Noisy wrapped phase maps obtained with the CMOS sensor could derive in false assumptions about the nature of such de-correlated patterns or the incapacity of the optical setup to perform the measurement. A remarkable result is that in high speed recording the performance of the sCMOS is better as it was expected, considering only the visualization and analysis of the phase maps and not only on SNR calculations. The methodology described in this report can be used to compare other top of technology on-chip image sensors such as the EM-CCD and it is complementary to the well-known SNR measurements.



This article is copyrighted as indicated in the article. Reuse of AIP content is subject to the terms at: http://scitation.aip.org/termsconditions. Downloaded to IP: 200.23.6.133 On: Thu, 03 Jul 2014 22:40:27

## ACKNOWLEDGMENTS

This research work was partially supported by the Consejo Nacional de Ciencia y Tecnología (CONACYT, grant 157053).

## REFERENCES

1. B. Moomaw, "Camera technologies for low light imaging: overview and relative advantages," in *Digital Microscopy*, edited by G. Sluder and D. E. Wolf, San Diego California: Elsevier, 2007, pp. 251-283.
2. J. R. Janesick, *Scientific charged coupled devices*, Bellingham Washington: SPIE, 2001, pp. 3-94.
3. M. Bigas, E. Cabruja, J. Forest and J. Salvi, *Microelectron J* **37**, 433-451 (2006).
4. S. Fullerton, K. Bennett, E. Toda and T. Takahashi, *Orca-flash 4.0, changing the game*, whitepaper, Hamamatsu Corp. (2011).
5. Z. Huang, H. Zhu, F. Long, H. Ma, L. Qin, Y. Liu, J. Ding, Z. Zhang, Q. Luo, and S. Zeng, *Opt. Express* **19**, 19156-19168 (2011).
6. H. T. Beier and B. L. Ibey, *PLoS One* **9**, e84614 (2014).
7. J. Jung, S. Weisenburger, S. Albert, D. F. Gilbert, O. Friedrich, V. Eulenburg, J. Kornhuber, and T. W. Groemer, *Microsc. Res. Techniq.* **76**, 835-846 (2013).
8. P. Qiu, YN. Mao, XM. Lu, E. Xiang, and XJ. Jiang, *Research in Astron. Astrophys.* **13**, 615-628 (2013).
9. C. Coates, *New sCMOS vs. current microscopy cameras*, whitepaper, Andor Tech. (2011).
10. J. Oreopoulos, A comparison of sCMOS and EMCCD digital camera technology for spinning disk confocal microscopy, whitepaper, Spectral applied research (2012).
11. Marchywka and D. G. Socker, *Appl. Opt.* **31**, 7198-7213 (1992).
12. A. M. Pozo and M. Rubiño, *Appl. Opt.* **44**, 1543-1547 (2005).
13. J. M. Flores-Moreno, C. Furlong, J. J. Rosowski, E. Harrington, J. T. Cheng, C. Scarpino, and F. Mendoza Santoyo, *Scanning* **33**, 342-352, (2011).
14. J. J. Rosowski, J. T. Cheng, M. E. Ravicz, N. Hulli, M. d S. Hernandez-Montes, E. Harrington, and C. Furlong, *Hear. Res.* **253**, 83-96 (2009).
15. P. Rastogi and D. Inaudi, *Trends in optical non-destructive testing and inspection*, San Diego California: Elsevier, 2000.
16. T. Kreis, *Handbook of Holographic Interferometry: optical and digital methods*, Weinheim: Wiley-VCH, 2005.
17. D. Robinson, *Interferogram analysis*, USA: IoP, 1993.
18. M. Takeda, H. Ina, and S. Kobayashi, *J. Opt. Soc. Am.* **72**, 156-160 (1982).



This article is copyrighted as indicated in the article. Reuse of AIP content is subject to the terms at: http://scitation.aip.org/termsconditions. Downloaded to IP: 200.23.6.133 On: Thu, 03 Jul 2014 22:40:27